JOURNAL OF SOLID STATE CHEMISTRY **128,** 282–288 (1997)
ARTICLE NO. SC967222

Synthesis and Characterization of Oxynitrides in the ZrO_2-Rich Part of the Systems Ca–Zr–O–N and Mg–Zr–O–N

M. Lerch,*,[1] J. Lerch,* R. Hock,† and J. Wrba†

*Lehrstuhl für Silicatchemie, Universität Würzburg, Röntgenring 10-11, 97070 Würzburg, Germany; and †Institut für Mineralogie, Universität Würzburg, Am Hubland, 97074 Würzburg, Germany

Received March 27, 1996; in revised form November 8, 1996; accepted November 12, 1996

Oxynitrides in the ZrO_2-rich part of the systems Ca–Zr–O–N and Mg–Zr–O–N have been prepared by nitridation of the corresponding oxides in nitrogen atmosphere at temperatures between 1400 and 2000°C. A thermodynamic model of the nitridation is presented. The crystal structures of the resulting oxynitride phases are derived from the fluorite-type structure of the cubic high temperature phase of ZrO_2. The structure of the β' phase in the Mg–Zr–O–N system has been investigated using X-ray powder methods. Its trigonally distorted fluorite-type structure (ordered anion vacancies) can be described by an arrangement of Bevan clusters (A_7X_{12} units) and A_7X_{14} units. At ~975°C, a transition into a cubic fluorite-type phase with randomly distributed vacancies has been observed.

INTRODUCTION

CaO- and MgO-stabilized zirconia ceramics are important materials due to their outstanding electrical and mechanical properties. Doping ZrO_2 with aliovalent oxides leads to the formation of oxygen vacancies. An alternative way to form anion vacancies in the zirconia lattice is the doping with Zr_3N_4. Cheng and Thompson (1) were the first who reported the direct nitridation of ZrO_2 in a nitrogen atmosphere at temperatures above 1400°C. The formation of anion vacancies can be described in the following way:

$$3O_O^x + N_2 = 2N_O' + V_O^{\circ\circ} + \tfrac{3}{2}O_2. \qquad [1]$$

The resulting β-type phases $ZrO_{2-2x}N_{4x/3}$ (ZrO_2–Zr_3N_4 system) show trigonally distorted fluorite-type structures with ordered anion vacancies. A summary of the known β-type phases and their structural details are given in some of our previous papers (2–4).

[1] To whom correspondence should be addressed.

Nitrogen incorporation into yttria-doped zirconia (Y–Zr–O–N system) by direct nitridation of yttria-stabilized zirconia was investigated by Thompson *et al.* (5–7).

The aim of the present work is the investigation of the ZrO_2-rich side of the systems Ca–Zr–O–N and Mg–Zr–O–N using samples containing different amounts of CaO/MgO and nitrogen. Details of vacancy ordering as a function of chemical parameters are given in another paper (8).

EXPERIMENTAL

Synthesis

Zirconia powder (Alfa, 99.9%) was mixed with MgO (Alfa, 99.9%) or $CaCO_3$ (Merck, 99.8%) in 2-propanol, dried, and pressed into pellets isostatically. The pellets were heated in air at 1750°C for 3 days. After grinding, XRD measurements were carried out for phase analysis. The prepared samples contained 1–15 mol % of the aliovalent dopant oxide. All zirconia pellets were nitrided in a graphite heated resistance furnace (T = 1400–1900°C, nitrogen pressure 1–6 bar, t = 2–4 h). Details are given in (8).

N/O Analysis

For N/O analysis, the method of hot gas extraction was used. After thermal decomposition of the samples in a graphite heated furnace at ~2700°C under helium atmosphere, the oxygen content was determined by measuring the CO_2 concentration (after oxidation of CO) with an IR-cell. Analysis of the nitrogen content was carried out by measuring the thermal conductivity of the mixture of helium and nitrogen gas after absorption of the CO_2. The accuracy is ~1% of the present N/O.

XRD Experiments

XRD investigations were carried out with a STOE STADIP powder diffractometer (Cu$K\alpha_1$ radiation,

0022-4596/97 $25.00

$\lambda = 154.06$ pm, position sensitive detector) and a Philips PW 1710 diffractometer (Cu$K\bar{a}$ radiation, $\lambda = 154.18$ pm, scintillation counter) equipped with a graphite secondary monochromator. For the high temperature measurements, a graphite heated resistance furnace was used (nitrogen atmosphere). Quantitative phase analysis was carried out using the polymorph method described by Garvie and Nicholson (9). The weight fraction of m-ZrO_2 (x_m) is given by:

$$x_m = \frac{I_m(111) + I_m(11\bar{1})}{I_m(111) + I_m(11\bar{1}) + I_c(111)}, \quad x_{\beta''} \approx x_c = 1 - x_m. \qquad [2]$$

I_m and I_c are the integrated intensities of the strongest reflections of monoclinic ZrO_2 and cubic zirconia; $x_{\beta''}$ and x_c represent the content of β'' and cubic phase, respectively. The β-type phases can be treated as cubic for these calculations. In order to prove the validity of this method, Rietveld refinements were carried out for some samples. The results of the simple polymorph method are in a good agreement with the results of the Rietveld refinement. The results only differ significantly in the case of very low contents of one phase (< 10 wt%). Lattice constants were determined using the program VISUAL X^{POW} (10). For the Rietveld refinements, the program packages WYRIET (11) and LHPM (12) were used. Parameters of data collection are summarized in Table 1. The profiles were fitted with a pseudo-Voigt function. R factors are defined in the following way:

$$R_{wp} = \sqrt{\frac{\sum w(y_{obs} - y_{calc})^2}{\sum w(y_{obs})^2}} \qquad R_{Bragg} = \frac{\sum |\text{“}I_{obs}\text{”} - I_{calc}|}{\sum \text{“}I_{obs}\text{”}}$$

$$R_{exp} = \sqrt{\frac{(N - P + C)}{\sum w(y_{obs})^2}} \qquad S = \frac{R_{wp}}{R_{exp}} \quad \text{(goodness of fit).}$$

TABLE 1
Parameters of Data Collection and Structural Parameters of the β' Phase $Zr_{0.878}Mg_{0.122}O_{1.68}N_{0.130}$

	$Zr_{6.15}Mg_{0.854}O_{11.8}N_{0.910}$
Formula mass	782.04 g/mol
Color	light brown
Crystal system	trigonal
Space group	$R\bar{3}$ (hexagonal setting)
Unit cell dimensions	$a = 953.35(7)$ pm
	$b = 953.35(7)$ pm
	$c = 1752.4(1)$ pm
	$\alpha = 90°$
	$\beta = 90°$
	$\gamma = 120°$
Cell volume	$V = 1379.46 \times 10^6$ pm^3
Formula units	$Z = 6$
Calculated density	$\rho = 5.65$ g/cm^3
Diffractometer	STOE STADIP
Wavelength	154.06 pm
Number of measured profile points	5251 (60 s/step)
	(position sensitive detector)
Two theta range	10°–116°
Number of refined parameters	34
R_{wp}	0.087
R_{Bragg}	0.087
R_{exp}	0.105
S	0.83

RESULTS AND DISCUSSION

Ca–Zr–O–N System

At temperatures above 1200°C, tetragonal and cubic high temperature phases exist in the ZrO_2-rich part of the systems Ca–Zr–O (13) and Zr–O–N (14). The concentration of anion vacancies plays an important role in the stability of the individual phases. During cooling to ambient temperature, the high temperature phases decompose into mixtures of monoclinic zirconia and a fluorite-type phase (Ca–Zr–O system) or a trigonally distorted fluorite type phase (β-type) with ordered anion vacancies (Zr–O–N system). Figure 1 presents the results of a quantitative phase analysis for the Ca–Zr–O system and two typical examples for the Ca–Zr–O–N system. In our experiments, a content of $\sim$14 mol% CaO is necessary to get pure cubic phase in the Ca–Zr–O system. With an increasing amount of nitrogen, obtained by a higher temperature of nitridation (1), the content of calcia necessary for the formation of pure cubic phase decreases strongly. At a nitridation temperature of 1900°C, the cubic phase is stabilized by only $\sim$4 mol% CaO. The stabilizing effects of calcia and nitrogen are additive! Samples in the region of small calcia and large nitrogen

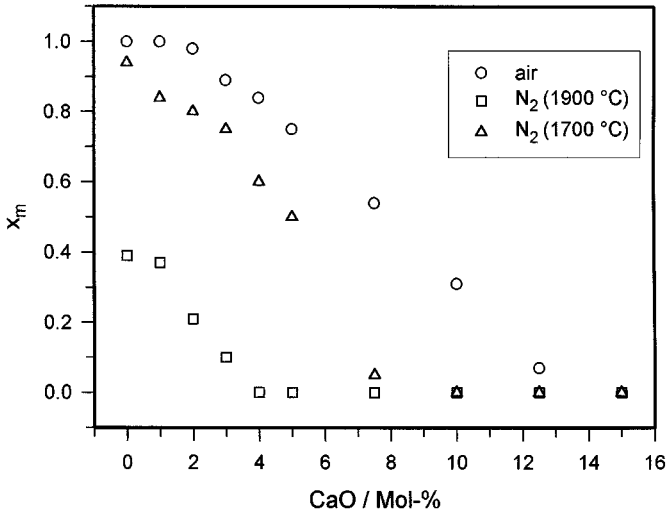

FIG. 1. Content of monoclinic phase as a function of the CaO concentration for different conditions of synthesis.

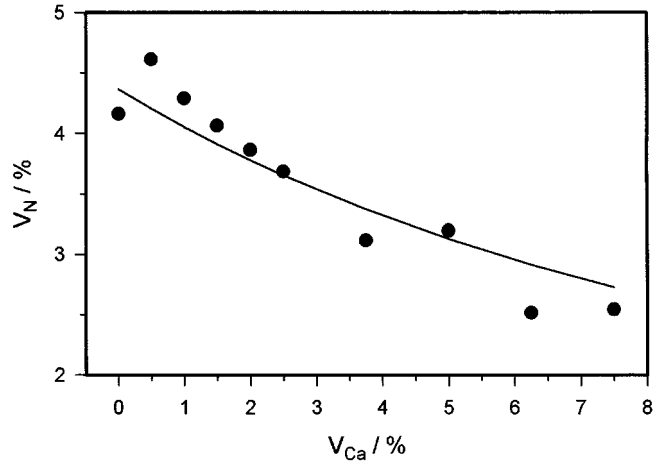

FIG. 2. Concentration of anion vacancies caused by nitrogen (V_N) as a function of the vacancy concentration caused by CaO (V_{Ca}) at a temperature of 1900°C (experimental and calculated data).

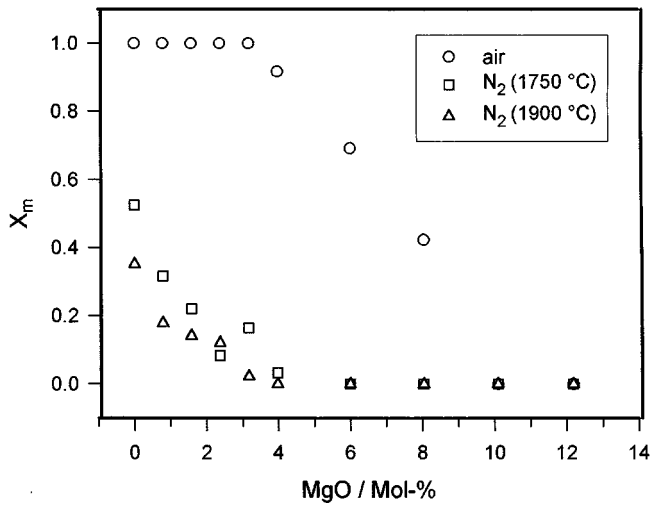

FIG. 4. Content of monoclinic phase as a function of the MgO concentration for different conditions of synthesis.

contents show an ordered arrangement of anion vacancies (β type phases), whereas randomly distributed vacancies can be observed for samples dominated by calcia (8). To describe this behavior, a term V_N/V_{total} is defined ($V_{total} = V_N + V_{Ca}$), where V_N and V_{Ca} can be calculated from $V_{N,Ca} = 100[V_O^{\circ\circ}]_{N,Ca}$. A V_N/V_{total} value below 0.65 leads to the formation of phases with randomly distributed anion vacancies. β-type phase structures can be observed for values above 0.65.

For a given temperature, the amount of incorporated nitrogen depends on the calcia concentration of the starting material. Increasing the CaO content leads to a decrease of the nitrogen concentration as shown in Fig. 2. In order to understand this behavior in a quantitative way, thermodynamic calculations were carried out, assuming a nearly ideal behavior of the defects at 1900°C. With the help of the law of mass action and Eq. [1], the nitridation of calcia doped zirconia can be described by

$$[N_O']^2[V_O^{\circ\circ}] = KP_{O_2}^{-3/2}P_{N_2}[O_O^x]^3, \qquad [3]$$

where

$$[V_O^{\circ\circ}] = [V_O^{\circ\circ}]_N + [V_O^{\circ\circ}]_{Ca}, \qquad [4]$$

with

$$[V_O^{\circ\circ}]_N = \tfrac{1}{2}[N_O'] \quad \text{and} \quad [V_O^{\circ\circ}]_{Ca} = [Ca_{Zr}''] \qquad [5]$$

($[N_O']$ and $[Ca_{Zr}'']$ can be determined experimentally),

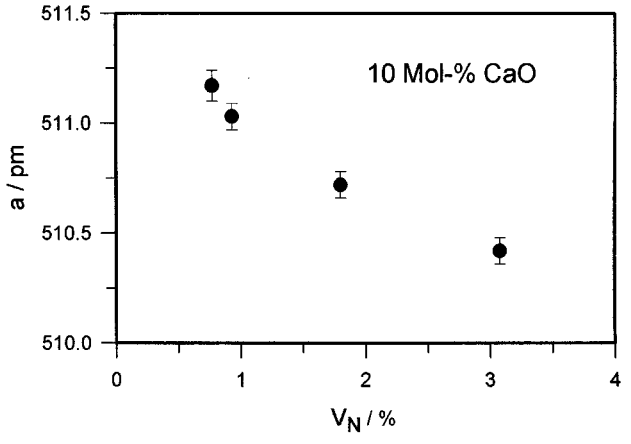

FIG. 3. Variation of the cell constant of cubic Zr–Ca–O–N phases for different amounts of nitrogen.

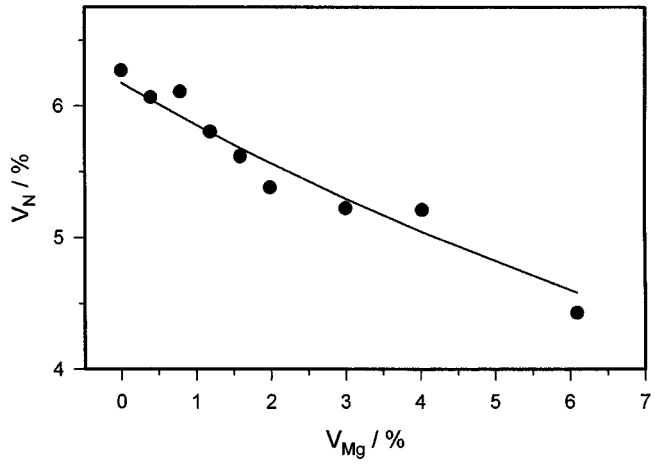

FIG. 5. Concentration of anion vacancies caused by nitrogen (V_N) as a function of the vacancy concentration caused by MgO (V_{Mg}) at a temperature of 1900°C (experimental and calculated data).

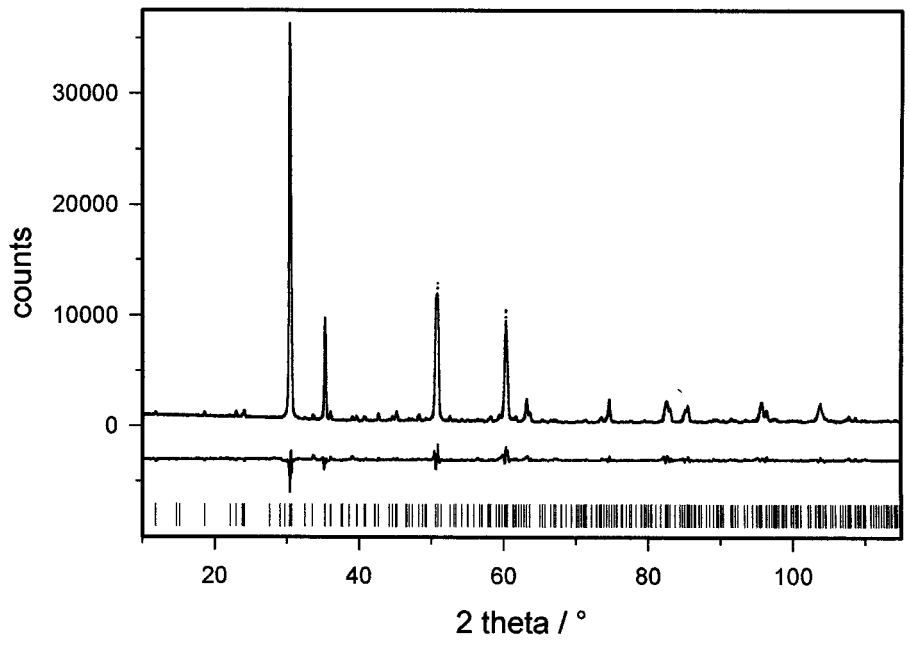

FIG. 6. X-ray powder diagram of the β' phase $Zr_{0.878}Mg_{0.122}O_{1.68}N_{0.130}$ and results of the Rietveld refinement.

and

$$[O_O^x] = [O_O^x]^* - 3[V_O^{\circ\circ}]_N - [V_O^{\circ\circ}]_{Ca}. \quad [6]$$

$[O_O^x]^*$ is the value in the case of pure ZrO_2. This leads to

$$KP_{O_2}^{-3/2}P_{N_2} = \frac{4[V_O^{\circ\circ}]_N^2[V_O^{\circ\circ}]_{Ca} + 4[V_O^{\circ\circ}]_N^3}{([O_O^x]^* - 3[V_O^{\circ\circ}]_N - [V_O^{\circ\circ}]_{Ca})^3}. \quad [7]$$

From kinetic investigations, it is known that equilibrium is reached after an annealing time of 4 h at 1900°C (14). The $[V_O^{\circ\circ}]_{Ca}$ and $[V_O^{\circ\circ}]_N$ values can be calculated easily from the CaO and nitrogen contents. Using a graphite heated furnace, the oxygen partial pressure for a given temperature is fixed and can be determined by thermodynamic calculations. The curve presented in Fig. 2 was fitted to the experimental data using a Marquardt–Levenberg algorithm (16) and the Newton method. There is an acceptable agreement between the measured and calculated data. K was refined to 2×10^{-25}.

The lattice constant of the cubic Ca–Zr–O phase increases with increasing CaO content. For a constant calcia concentration, the lattice parameter decreases with increasing nitrogen content, as shown in Fig. 3. This behavior is

TABLE 2
Refined Parameters of the β' Phase $Zr_{0.878}Mg_{0.122}O_{1.68}N_{0.130}$

Atom	x	y	z	B_{iso}[a]	Zr/Mg ratio
Zr/Mg 1	0	0	0	0.70	0.86(5)/0.14(5)
Zr/Mg 2	0.2177(3)	0.2584(3)	0.1731(2)	0.53	0.86(3)/0.14(3)
Zr/Mg 3	0.2385(3)	0.0480(5)	0.3275(2)	0.88	0.86(3)/0.14(3)
Zr/Mg 4	0	0	1/2	0.70	0.84(5)/0.16(5)
O/N 1	0.230(3)	0.062(3)	0.450(1)	0.90	
O/N 2	0.213(2)	0.248(2)	0.297(2)	0.90	
O/N 3	0.212(2)	0.042(3)	0.201(1)	0.90	
O/N 4	0.195(3)	0.194(3)	0.055(1)	0.90	
O/N 5	0	0	0.357(2)	0.90	

[a] Not refined, values taken from $Zr_5Sc_2O_{13}$ [21].

TABLE 3
Selected Bond Lengths (pm) in the β' Phase $Zr_{0.878}Mg_{0.122}O_{1.68}N_{0.130}$

Zr/Mg 1–O/N 4	209	Zr/Mg 2–O/N 3	209
Zr/Mg 1–O/N 4	209	Zr/Mg 2–O/N 4	214
Zr/Mg 1–O/N 4	209	Zr/Mg 2–O/N 2	217
Zr/Mg 1–O/N 4	209	Zr/Mg 2–O/N 1	220
Zr/Mg 1–O/N 4	209	Zr/Mg 2–O/N 3	223
Zr/Mg 1–O/N 4	209	Zr/Mg 2–O/N 3	223
		Zr/Mg 2–O/N 1	224
Zr/Mg 3–O/N 2	209	Zr/Mg 4–O/N 1	215
Zr/Mg 3–O/N 2	211	Zr/Mg 4–O/N 1	215
Zr/Mg 3–O/N 4	212	Zr/Mg 4–O/N 1	215
Zr/Mg 3–O/N 5	215	Zr/Mg 4–O/N 1	215
Zr/Mg 3–O/N 1	215	Zr/Mg 4–O/N 1	215
Zr/Mg 3–O/N 3	223	Zr/Mg 4–O/N 1	215
Zr/Mg 3–O/N 2	233	Zr/Mg 4–O/N 5	251
Zr/Mg 3–O/N 4	273	Zr/Mg 4–O/N 5	251

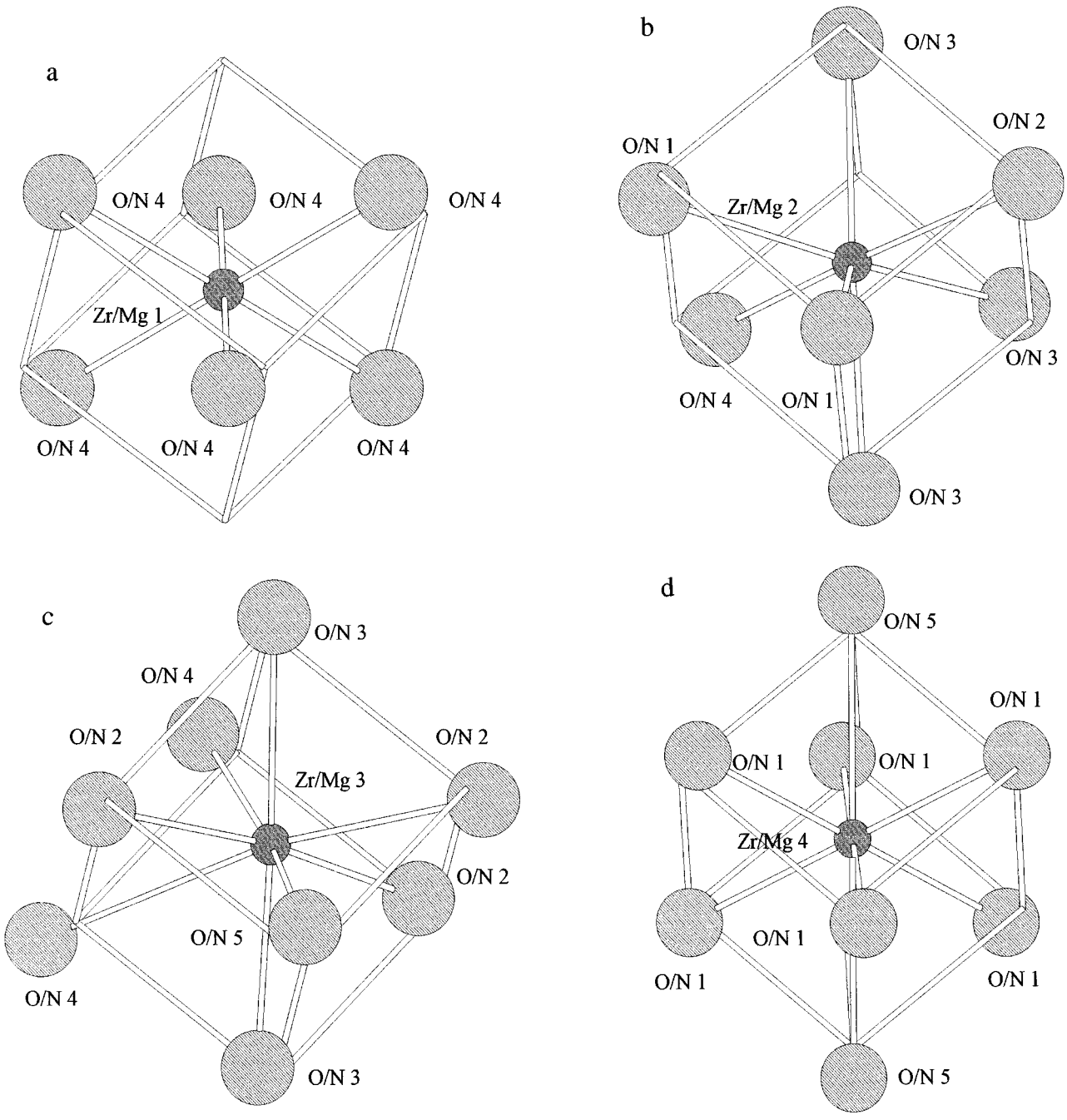

FIG. 7. Zr/Mg coordination polyhedra in $Zr_{0.878}Mg_{0.122}O_{1.68}N_{0.130}$ (20). The cubes represent the ideal fluorite structure.

similar to that of oxynitrides in the Y–Zr–O–N system, described by Cheng and Thompson (5).

Mg–Zr–O–N System

Similar investigations were carried out in the Mg–Zr–O–N system. Again, the stabilizing effects of nitrogen and the aliovalent cation are additive (Fig. 4). About 10 mol% of MgO are necessary to completely suppress the formation of the monoclinic phase in the Mg–Zr–O system. This value can be decreased to ~ 4 mol% MgO in the Mg–Zr–O–N system if a nitridation temperature of 1900°C is used. Higher temperatures of the nitridation ($T \geq 2000$°C) lead to the formation of rock salt-type intercalation phases derived from ZrN.

The amount of incorporated nitrogen decreases with an increasing content of MgO (Fig. 5). This behavior can be

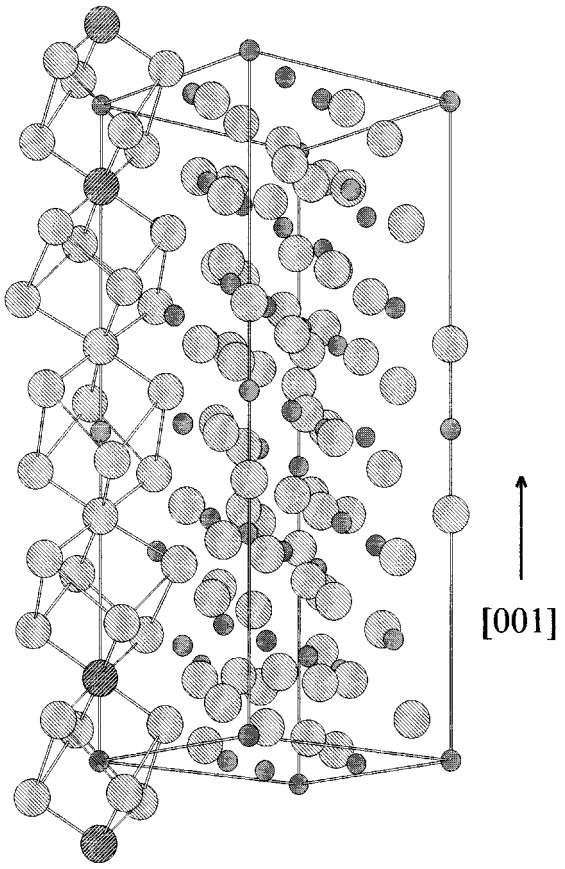

FIG. 8. Structure plot of the β' phase unit cell (20). Cations are shown as small circles, anions as light large circles, and some selected anion vacancies as dark large circles.

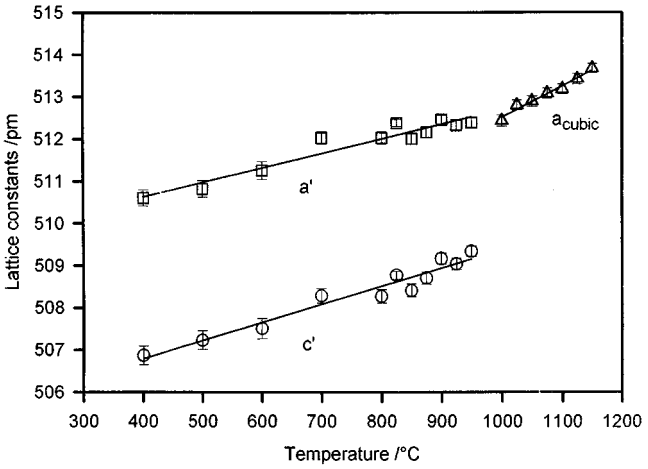

FIG. 9. Lattice constants of $Zr_{0.878}Mg_{0.122}O_{1.68}N_{0.130}$ as a function of the temperature ($a' = a_h/\sqrt{7/2}$, $c' = c_h/2\sqrt{3}$).

described using the model presented for the Ca–Zr–O–N system. Again, the calculated data are in good agreement with the experimental results. K was refined to 1×10^{-25}, which is very similar compared with the value of the Ca–Zr–O–N system.

In contrast to the Ca–Zr–O–N system, where phases with ordered anion vacancies are observed only above a V_N/V_{total} value of 0.65, β-type phases exist up to 12 mol% MgO and probably even higher concentrations in the Mg–Zr–O–N system. Above a V_N/V_{total} value of 0.96 the β'' phase forms, known from the Zr–O–N system (1–4, 14, 15). With increasing content of MgO, the β' phase becomes stable. This type of trigonally distorted fluorite-type structure is known in the Mg–Zr–O system ($MgZr_6O_{13}$). As a minor phase it is only detectable by electron diffraction (13) and occurs as well in the Zr–O–N system as a highly disordered and metastable phase (4, 14, 17). The synthesis of nearly pure β' phase without monoclinic zirconia as a secondary phase is possible only in the Mg–Zr–O–N system. For the structural investigations, a sample without the monoclinic phase was chosen. Its composition is $Zr_{0.878}Mg_{0.122}O_{1.68}N_{0.130}$. As shown by TEM investigations, the amount of amorphous phases is small.

The β' phase crystallizes in space group $R\bar{3}$ (e.g., 18, 22, 23). The lattice parameters (hexagonal setting) were refined to $a = 953.35(7)$ pm and $c = 1752.4(1)$ pm. Starting parameters for the Rietveld refinement were taken from the structure determination of the β' phase in the ZrO_2–Zr_3N_4 system (18). Figure 6 shows the powder diagram of $Zr_{0.878}Mg_{0.122}O_{1.68}N_{0.130}$ with the final results of the refinement (calculated diagram and difference plot $I_{obs} - I_{calc}$). Structural parameters are given in Table 2; bond lengths are shown in Table 3. No large differences between the observed and calculated profile can be observed and the goodness of fit is acceptable (see Table 1). The absence of a large amount of monoclinic ZrO_2 is one of the reasons for the better quality of the structure determination compared with the metastable and highly disordered β' phase in the Zr–O–N system ($Zr_7O_{11}N_2$), which can be synthesized only with large amounts of monoclinic ZrO_2 as a secondary phase (4, 18). The crystal structure is made up by two basic building units: a A_7X_{12} unit, the so-called Bevan cluster (19), and a A_7X_{14} unit, which is very similar to the basic building unit of cubic ZrO_2. All zirconium/magnesium atoms of the A_7X_{14} unit (Zr/Mg 3, Zr/Mg 4) have an eightfold coordination (seven edge-shared AX_8 cubes), Zr/Mg 3 should better be described as 7 + 1 coordinated, the central atom of the Bevan cluster (Zr/Mg 1) a sixfold coordination, and the other atoms (Zr/Mg 2) of the Bevan cluster a sevenfold coordination. The polyhedra are shown in Fig. 7. The structure can be described by an alternated, edge-shared stacking of equal numbers of these basic building units in the [001] direction (Fig. 8), whereas the anion vacancies are ordered along [001] which corresponds to the [111] direction of the former cubic lattice. There are three AX_8/A_7X_{14} strings along [001] in the hexagonal setting of

the unit cell; further strings not shown in Fig. 8 are shifted by translations 1/3 2/3 2/3 and 2/3 1/3 1/3, respectively. The β' phase in the Mg–Zr–O–N system crystallizes isostructurally to, e.g., $Zr_5Sc_2O_{13}$, as reported by Thornber *et al.* (21). However, the deviations of the atomic coordinates from the ideal fluorite positions are smaller for the β' phase than for most atoms in $Zr_5Sc_2O_{13}$. A detailed explanation of these deviations on the basis of electrostatic grounds is given by Thornber *et al.* (21). The refined crystal structure is also in good agreement with the structure of $Zr_7O_{11}N_2$ suggested by Gilles (22) and Collongues *et al.* (23). Furthermore, it represents the hypothetical $n = 14$ structure type of the R_nO_{2n-2} series of rare earth oxides, as reported by Eyring and co-workers (e.g., 24, 25). This structure type was not observed yet in the binary rare earth oxide systems. No indication for Zr/Mg ordering was found in the Rietveld refinement of the X-ray data (see Table 2). This can be explained by the low mobilities of the cations. Thus, cation ordering in this type of fluorite structures is kinetically controlled (e.g., 13). In contrast, the anion mobilities are very large in nitrogen-containing zirconia materials (14). Pauling's 2nd rule points to an N/O ordering, preferring nitrogen on the anion site around the central atom of the Bevan cluster (O/N 4), which cannot be investigated with X-ray methods. Hence, neutron scattering experiments are in preparation.

The high temperature behavior of the β' phase in the Mg–Zr–O–N system was investigated by XRD-measurements up to a temperature of 1150°C in a nitrogen atmosphere. In contrast to the metastable β' phase in the ZrO_2–Zr_3N_4 system, decomposing irreversible to the β'' phase and monoclinic ZrO_2 at $\sim$800°C (13), the MgO containing β' phase shows a reversible transition into a cubic fluorite type high temperature phase with randomly distributed vacancies at $\sim$975°C. Above this temperature, the material may be of interest as an anion conductor. The lattice parameters as a function of temperature are shown in Fig. 9. For a better comparison with the cubic high temperature structure, the trigonal lattice parameters (hexagonal setting) are expressed as $a' = a_h/\sqrt{7/2}$ and $c' = c_h/2\sqrt{3}$. At 975°C the lattice constants a' and a_{cubic} are similar. Only c' increases immediately to the size of a_{cubic}. The linear thermal expansion coefficients of the β' phase are $\alpha_{a'} = 6.714(4) \times 10^{-6}\,K^{-1}$ and $\alpha_{c'} = 8.497(6) \times 10^{-6}\,K^{-1}$ between 400 and 950°C. The larger thermal expansion coefficient of the cubic high temperature phase with $\alpha_{a(cubic)} = 14.634(7) \times 10^{-6}\,K^{-1}$ between 1000 and 1150°C is equal to the coefficient of pure MgO stabilized zirconia (no nitrogen) with $\alpha_{a(cubic)} = 14.62(1) \times 10^{-6}\,K^{-1}$.

ACKNOWLEDGMENTS

Many thanks to Prof. G. Müller and the Deutsche Forschungsgemeinschaft (DFG) for financial support.

REFERENCES

1. Y. B. Cheng and D. P. Thompson, *Special Ceram.* **9,** 149 (1992).
2. M. Lerch, R. Hock, and E. Füglein, *Z. Kristallogr. Suppl.* **9,** 193 (1995).
3. R. Hock, M. Lerch, K. S. Knight, and H. Boysen, *Z. Kristallogr. Suppl.* **9,** 298 (1995).
4. M. Lerch, F. Krumeich, and R. Hock, submitted for publication.
5. Y. B. Cheng and D. P. Thompson, *J. Am. Ceram. Soc.* **76**(3), 683 (1993).
6. Y. B. Cheng and D. P. Thompson, *J. Am. Ceram. Soc.* **74**(5), 1135 (1991).
7. B. A. Shaw, Y. B. Cheng, and D. P. Thompson, *in* "Engineering Ceramics—Fabrication Science & Technology, Brit. Ceram. Proc., No. 50" (D. P. Thompson, Ed.), pp. 143–152. Institute of Materials, 1993.
8. M. Lerch J. Wrba, and J. Lerch, *J. Solid State Chem.*, in press.
9. R. C. Garvie and P. S. Nicholson, *J. Am. Ceram. Soc.* **55** (6), 303 (1972).
10. Stoe, "Visual X^{POW}", Darmstadt, 1994.
11. J. Schneider, "Wyriet", Version 3, Pöcking, 1994.
12. R. J. Hill and C. J. Howard, Report AAECM112, Australian Atomic Energy Commission, Lucas Heights Research Laboratories, New South Wales, Australia, 1986.
13. V. S. Stubican, "Science and Technology of Zirconia III 71" Advances in Ceramics, Vol. 24, (1988).
14. M. Lerch and O. Rahäuser, *J. Mater. Sci.*, in press.
15. M. Lerch, *J. Am. Ceram. Soc.*, in press.
16. D. W. Marquardt, *J. Soc. Ind. Appl. Math.* **11,** 431 (1963).
17. G. Van Tendeloo and G. Thomas, *Acta Metall.* **31,** 1611 (1983).
18. E. Füglein, R. Hock, M. Lerch, and H. Boysen, submitted for publication.
19. B. Hudson and P. T. Mosely, *J. Solid State Chem.* **19,** 383 (1976).
20. G. Thiele, "Moplo", Verlag Chemie, Weinheim, 1993.
21. M. R. Thornber, D. J. M. Bevan, and J. Graham, *Acta Crystallogr.* **B 24**, 1183 (1968).
22. J. C. Gilles, *Bull. Soc. Chim. Fr.* **22,** 2118 (1962).
23. R. Collongues, J. C. Gilles, A. M. Lejus, M. Perez, Y. Yorba, and D. Michel, *Mater. Res. Bull.* **2,** 837 (1967).
24. Z. C. Kang, J. Zhang, and L. Eyring, *Z. Anorg. Allg. Chem.* **622,** 465 (1996).
25. P. Kunzmann and L. Eyring, *J. Solid State Chem.* **14,** 229 (1975).